Supporting Information

New Homoleptic Gold Carbene Complexes via Ag-Au Transmetalation: Synthesis and Application of the $[Au(diNHC)_2]^{3+}$ Cations as ^{1}H-NMR and UV-vis Halides Sensors

Marco Baron,*[a] Anna Dall'Anese,[a] Alessandro Miolato,[a] Maddalena L. C. Cairoli,[a] Valerio Di Marco,[a] Claudia Graiff,[b] Alexander Pöthig[c] and Cristina Tubaro*[a]

[a] Dipartimento di Scienze Chimiche, Università degli Studi di Padova, via Marzolo 1; 35131 Padova, Italy.
E-mail: marco.baron@unipd.it; cristina.tubaro@unipd.it
[b] Dipartimento di Scienze Chimiche, della Vita e della Sostenibilità Ambientale, Università degli Studi di Parma, Parco Area delle Scienze 17/A, 43124 Parma, Italy.
[c] Department of Chemistry and Catalysis Research Center, Technical University of Munich, Lichtenbergstraße 4, Garching, 85747, Germany.

1. NMR spectra of compound $[AuL^3_2](PF_6)_3$

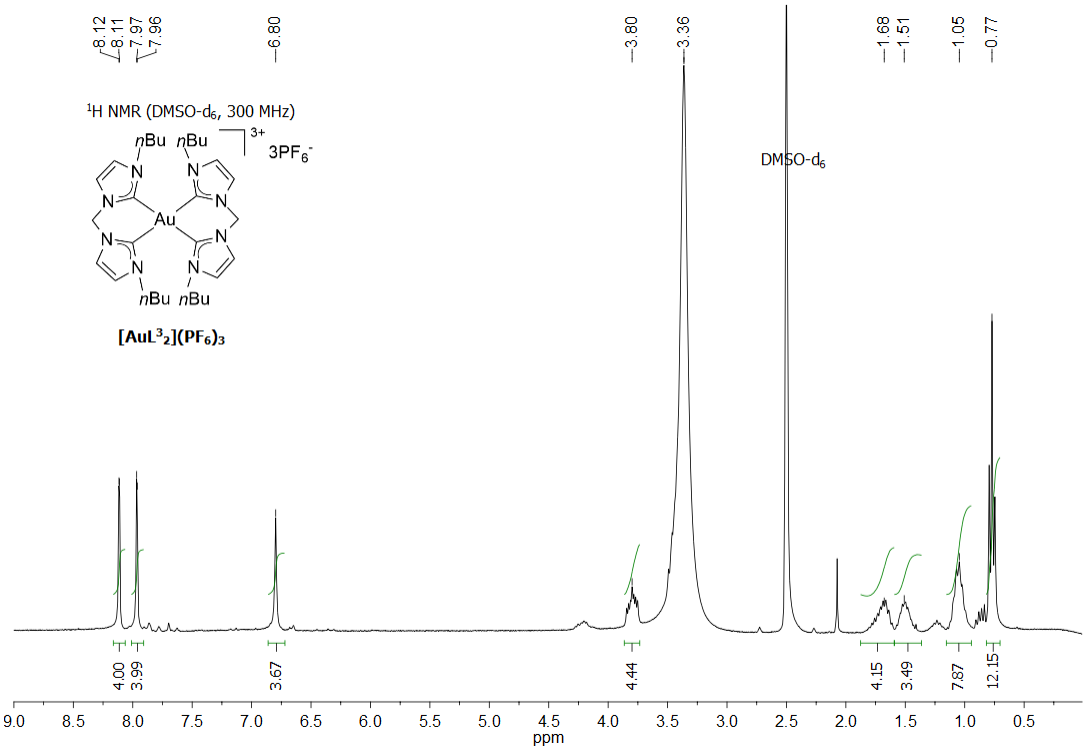

Figure S1: ^{1}H NMR (DMSO-d$_6$, 300 MHz) of **$[AuL^3_2](PF_6)_3$**.

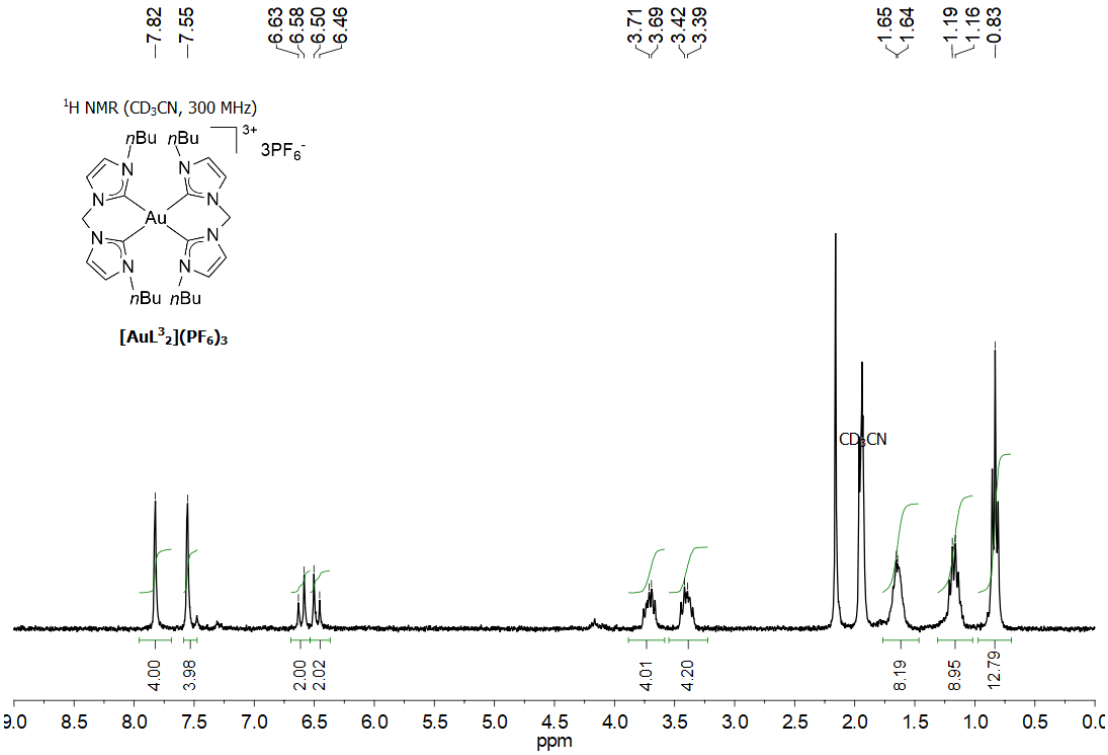

Figure S2: ^{1}H NMR (CD$_3$CN, 300 MHz) of **$[AuL^3_2](PF_6)_3$**.

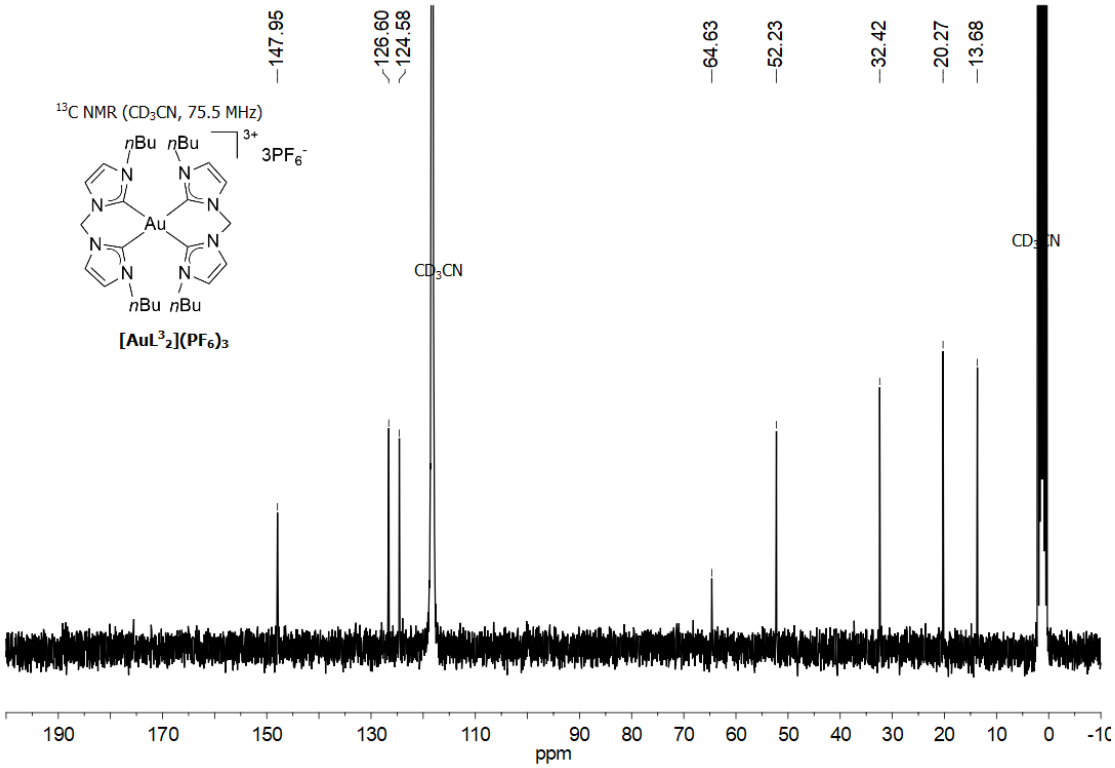

Figure S3: $^{13}C\{^{1}H\}$ NMR (CD_3CN, 75.5 MHz) of **[AuL$^3_2$](PF$_6$)$_3$**.

2. NMR spectra of compound $[AuL^4_2](PF_6)_3$

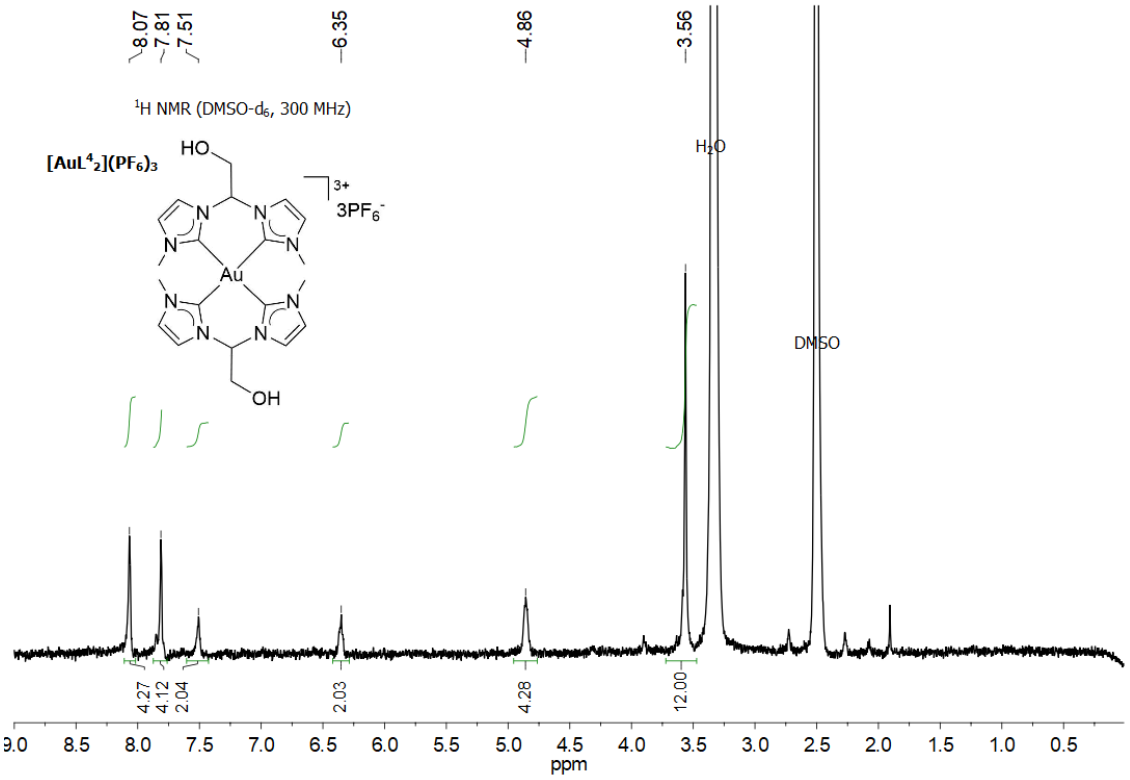

Figure S4: ^{1}H NMR (DMSO-d$_6$, 300 MHz) of **$[AuL^4_2](PF_6)_3$**.

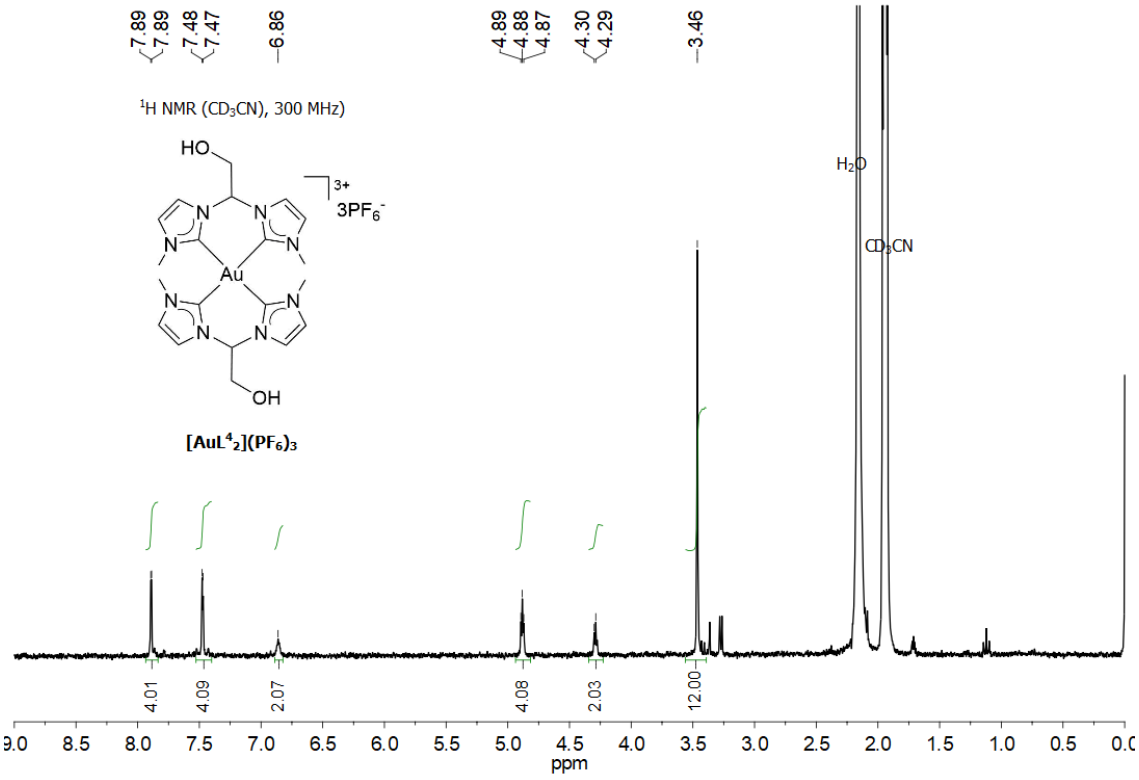

Figure S5: ^{1}H NMR (CD$_3$CN, 300 MHz) of **$[AuL^4_2](PF_6)_3$**.

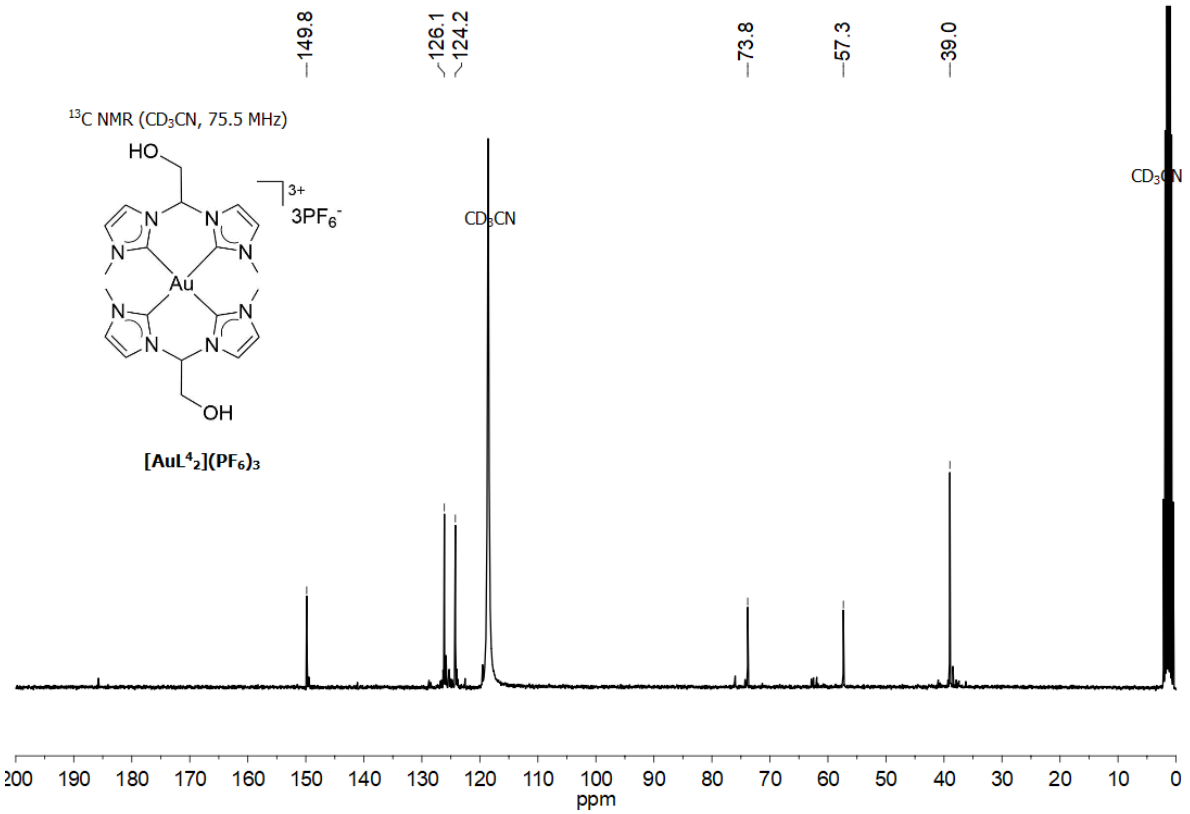

Figure S6: $^{13}C\{^{1}H\}$ NMR (CD_3CN, 75.5 MHz) of **[AuL$^4_2$](PF$_6$)$_3$**.

3. NMR spectra of compound $[Au_2L^7_2](BF_4)_2$

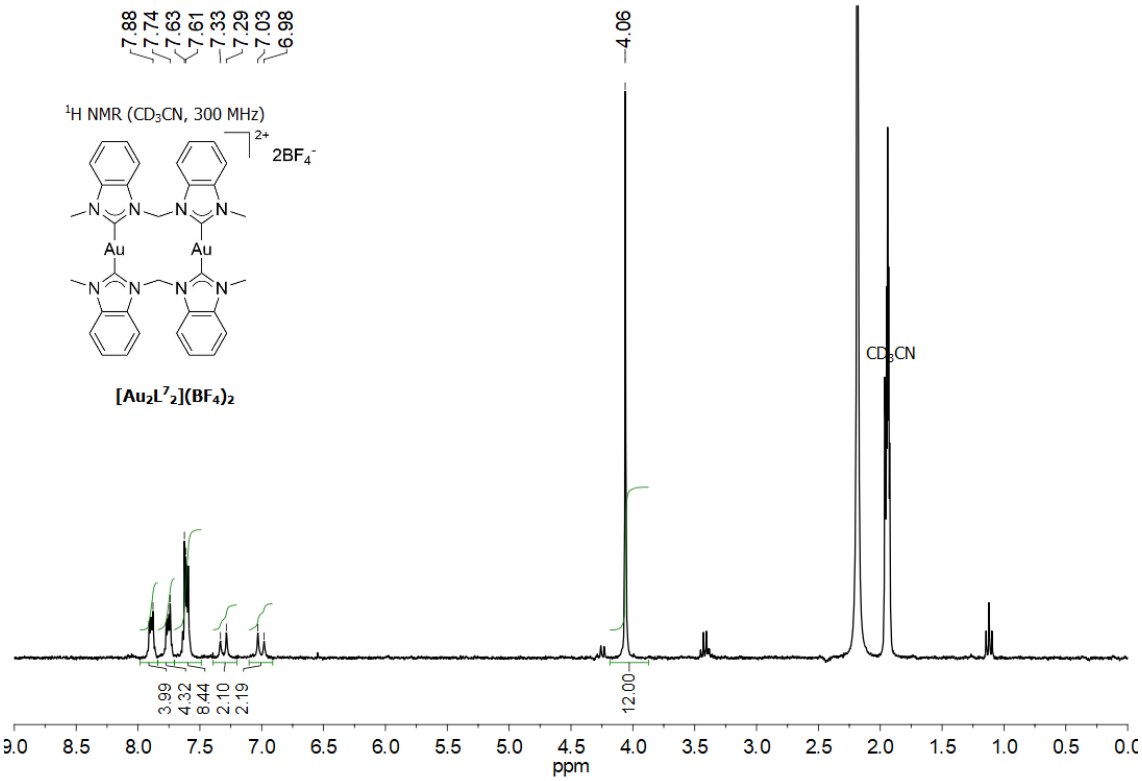

Figure S7: ^{1}H NMR (CD_3CN, 300 MHz) of $[Au_2L^7_2](BF_4)_2$

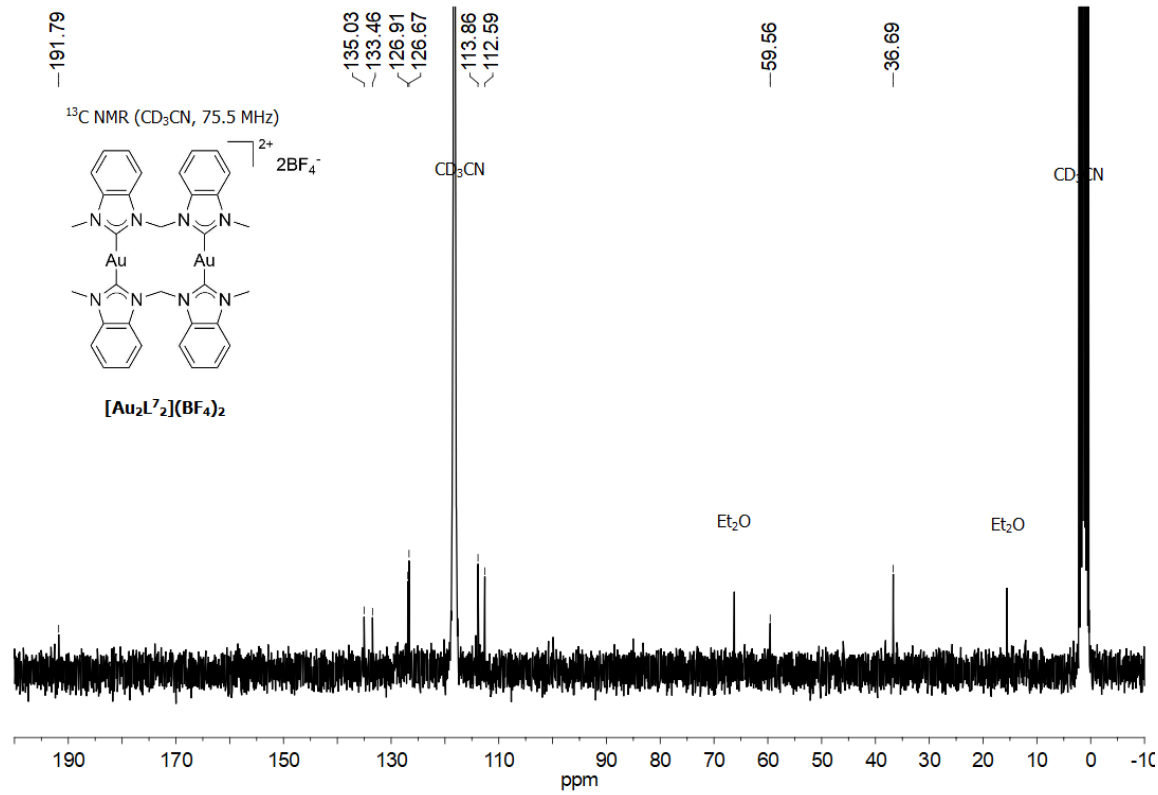

Figure S8: ^{13}C{1H} NMR (CD_3CN, 75.5 MHz) of $[Au_2L^7_2](BF_4)_2$.

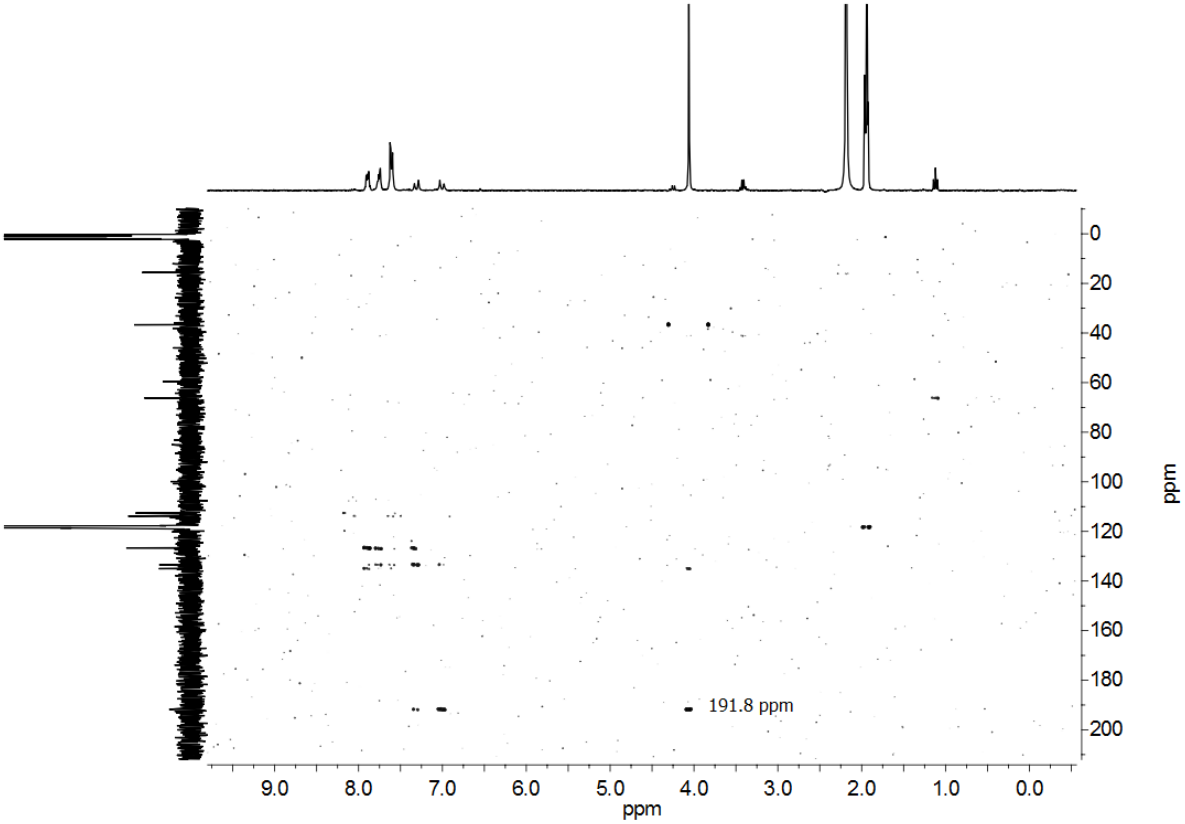

Figure S9: Section of the $^{1}H,^{13}C$ HMBC NMR (CD_3CN) of **$[Au_2L^7_2](BF_4)_2$**, showing the carbene carbon.

4. NMR titration of $Et_4NCl{\cdot}H_2O$ to $[AuL^3{}_2](PF_6)_3$ in DMSO-*d_6* (*Method A*)

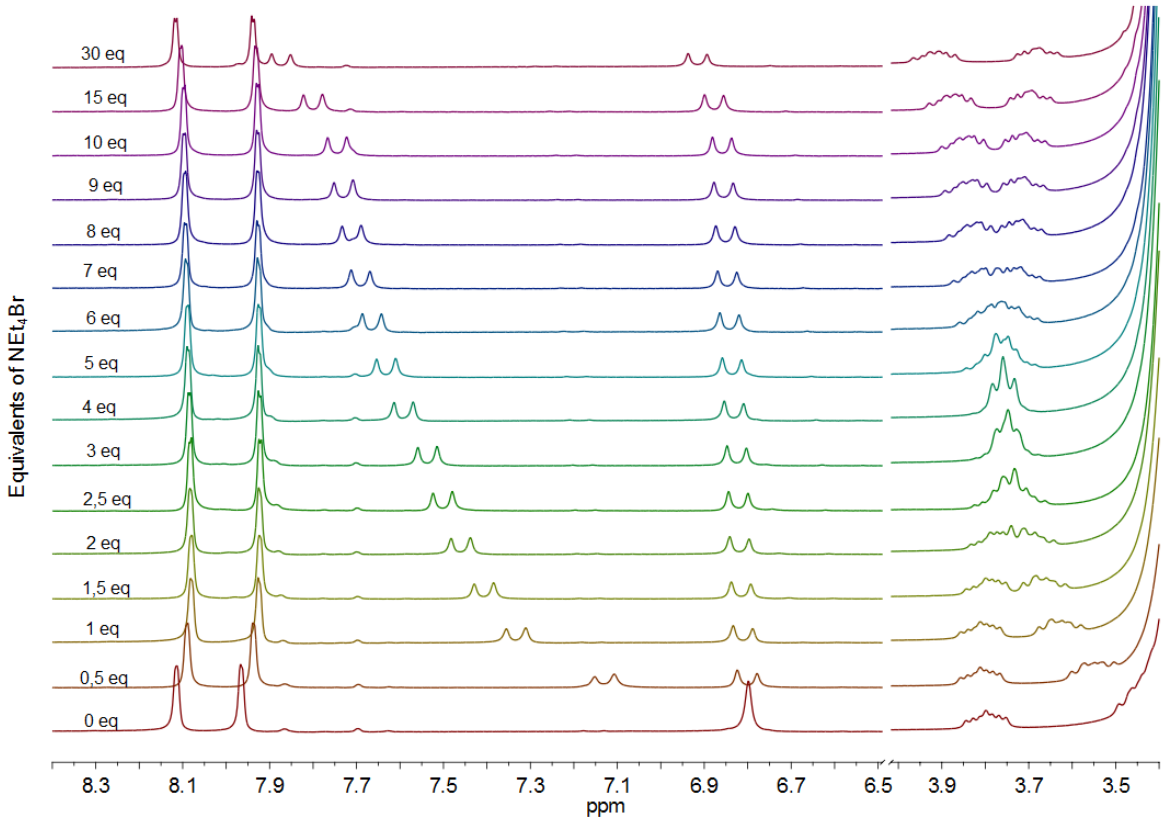

Figure S10: ^{1}H NMR titration (300 MHz, 298 K) of $Et_4NCl{\cdot}H_2O$ in DMSO-d_6 into a $4.34{\cdot}10^{-3}$ M solution of **$[AuL^3{}_2](PF_6)_3$** in DMSO-d_6.

Table S1: ^{1}H NMR titration (300 MHz, 298 K) data of $Et_4NCl{\cdot}H_2O$ in DMSO-d_6 into a $4.34{\cdot}10^{-3}$ M solution of **$[AuL^3{}_2](PF_6)_3$** in DMSO-d_6.

$[Au]_0$ (mM)	$[Cl^-]_0$ (mM)	$[Cl^-]_0/[Au]_0$	δ HA (ppm)	Δδ HA (ppm)	δ CH_2 X A (ppm)	δ CH_2 X B (ppm)
4.340	0	0	6.797	0	nd	nd
4.318	2.159	0.5	7.188	0.408	3.5647	3.8287
4.297	4.297	1	7.367	0.588	3.6327	3.837
4.276	6.414	1.5	7.475	0.686	3.6782	3.807
4.255	8.510	2	7.546	0.748	3.7259	3.7927
4.234	10.59	2.5	7.595	0.791	3.7575	3.7718
4.214	12.64	3	7.64	0.827	3.7762	3.7762
4.173	16.69	4	7.698	0.874	3.7813	3.7952
4.133	20.67	5	7.74	0.906	3.8018	3.7808
4.094	24.57	6	7.782	0.936	3.8237	3.7652
4.056	28.39	7	7.802	0.949	3.8332	3.7557
4.019	32.15	8	7.826	0.964	3.8552	3.7432
3.982	35.83	9	7.846	0.976	3.8659	3.7324
3.945	39.45	10	7.865	0.987	3.8844	3.7281
3.774	56.61	15	7.914	1.008	3.9081	3.7171
3.338	100.2	30	7.997	1.013	3.947	3.709

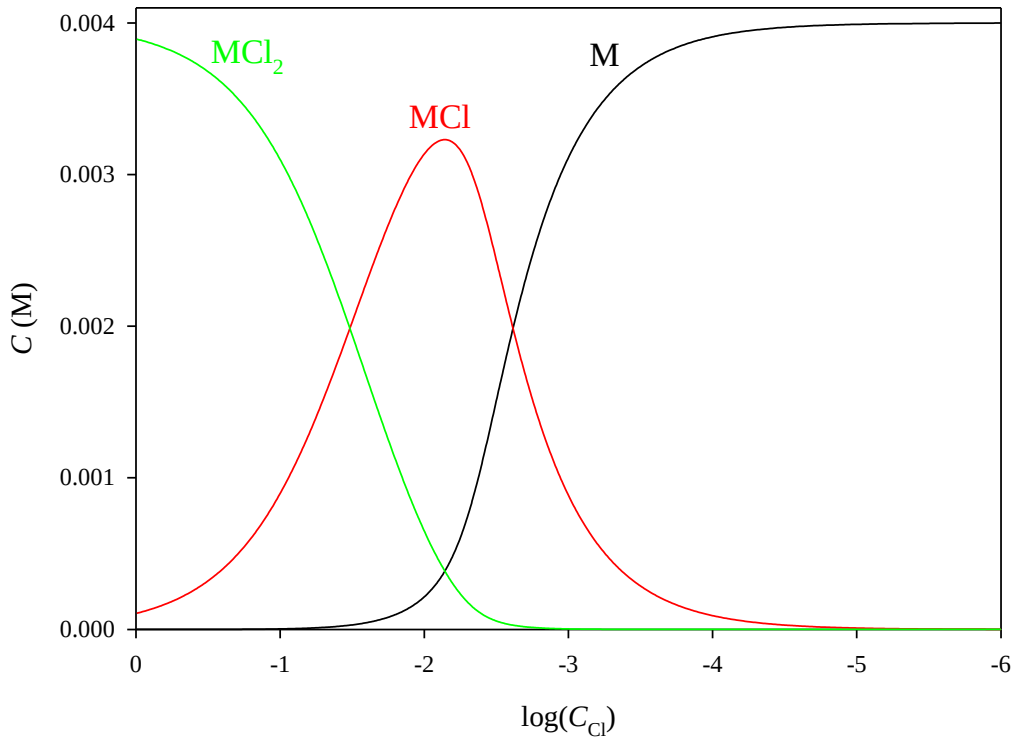

Figure S11: Species distribution diagram versus the total concentration of chloride for 0.0004 M host solution (M = $\mathbf{[AuL^3{}_2]^{3+}}$, MCl = $\mathbf{[AuClL^3{}_2]^{2+}}$, MCl_2 = $\mathbf{[AuCl_2L^3{}_2]^{+}}$).

5. NMR titration of Et_4NBr to $[AuL^3{}_2](PF_6)_3$ in DMSO-d_6 (*Method A*)

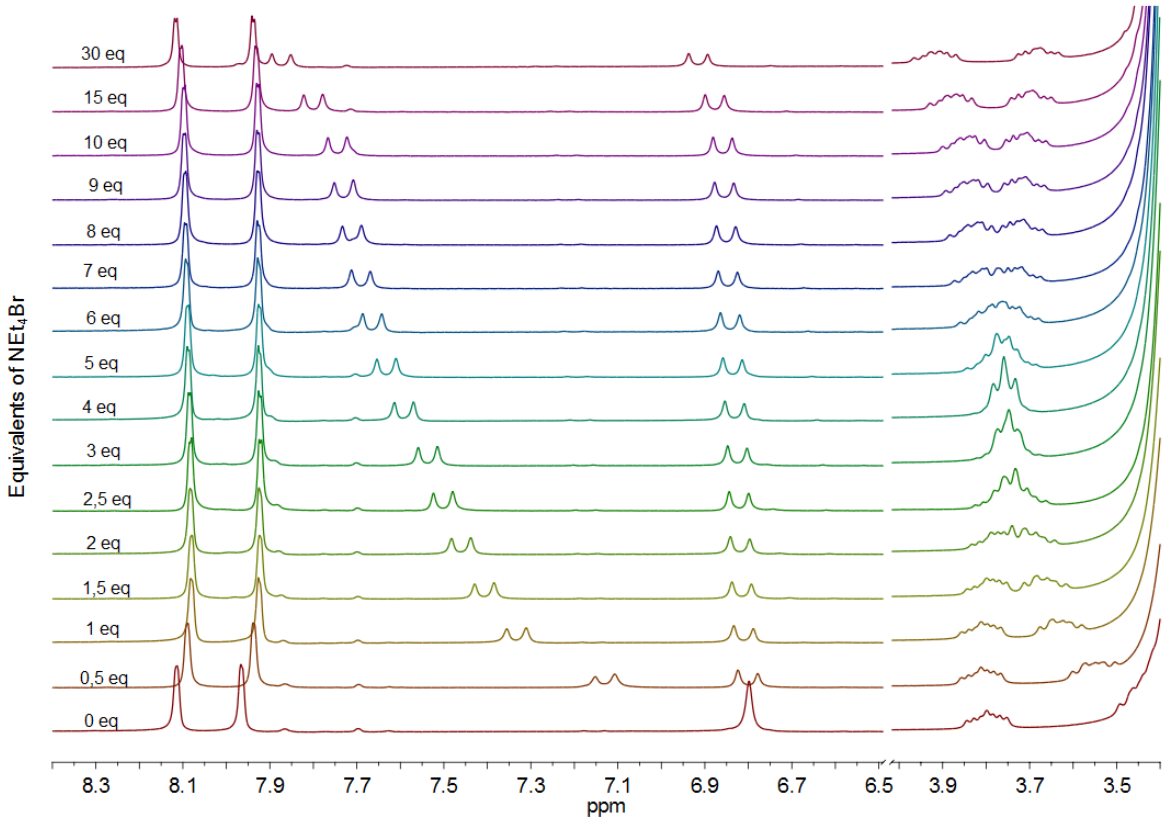

Figure S12: ^{1}H NMR titration (300 MHz, 298 K) of EtN_4Br in DMSO-d_6 into a $4.60 \cdot 10^{-3}$ M solution of **$[AuL^3{}_2](PF_6)_3$** in DMSO-d_6.

Table S2: ^{1}H NMR titration (300 MHz, 298 K) data of Et_4NBr in DMSO-d_6 into a $4.60 \cdot 10^{-3}$ M solution of **$[AuL^3{}_2](PF_6)_3$** in DMSO-d_6.

$[Au]_0$ (mM)	$[Br^-]_0$ (mM)	$[Br^-]_0/[Au]_0$	δ HA (ppm)	Δδ HA (ppm)	δ CH_2 X A (ppm)	δ CH_2 X B (ppm)
4.600	0.000	0.00	6.798	0	nd	nd
4.577	2.305	0.50	7.129	0.328	3.558	3.811
4.554	4.588	1.01	7.333	0.523	3.631	3.812
4.532	6.848	1.51	7.407	0.591	3.669	3.791
4.510	9.086	2.01	7.46	0.651	3.69	3.78
4.488	11.30	2.52	7.502	0.681	3.716	3.775
4.466	13.50	3.02	7.537	0.712	3.741	3.768
4.423	17.82	4.03	7.592	0.761	3.759	3.759
4.381	22.07	5.04	7.634	0.798	3.765	3.755
4.340	26.23	6.04	7.665	0.823	3.775	3.746
4.299	30.32	7.05	7.69	0.843	3.784	3.735
4.259	34.33	8.06	7.712	0.861	3.806	3.713
4.220	38.26	9.07	7.73	0.875	3.824	3.704
4.182	42.13	10.07	7.744	0.885	3.841	3.698
4.000	60.44	15.11	7.8	0.923	3.869	3.684
3.538	106.9	30.22	7.874	0.958	3.912	3.672

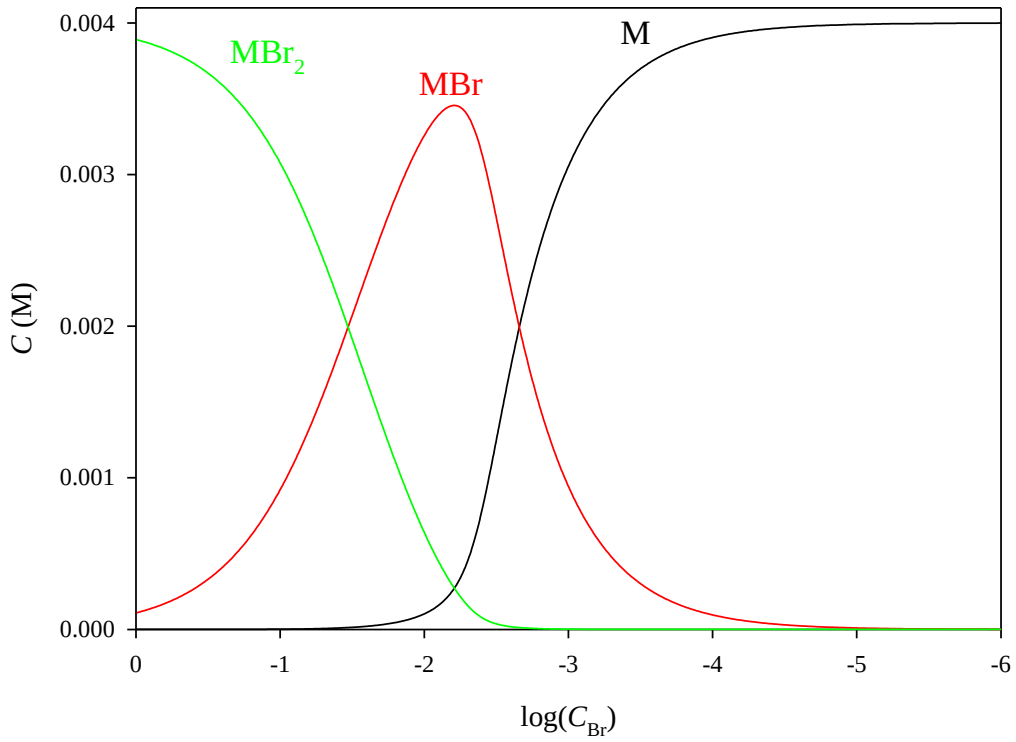

Figure S13: Species distribution diagram versus the total concentration of bromide for 0.0004 M host solution (M = $\mathbf{[AuL^3{}_2]^{3+}}$, MBr = $\mathbf{[AuBrL^3{}_2]^{2+}}$, MBr_2 = $\mathbf{[AuBr_2L^3{}_2]^{+}}$).

6. NMR titration of Bu_4NI to $[AuL^3_2](PF_6)_3$ in DMSO-d_6 (*Method A*)

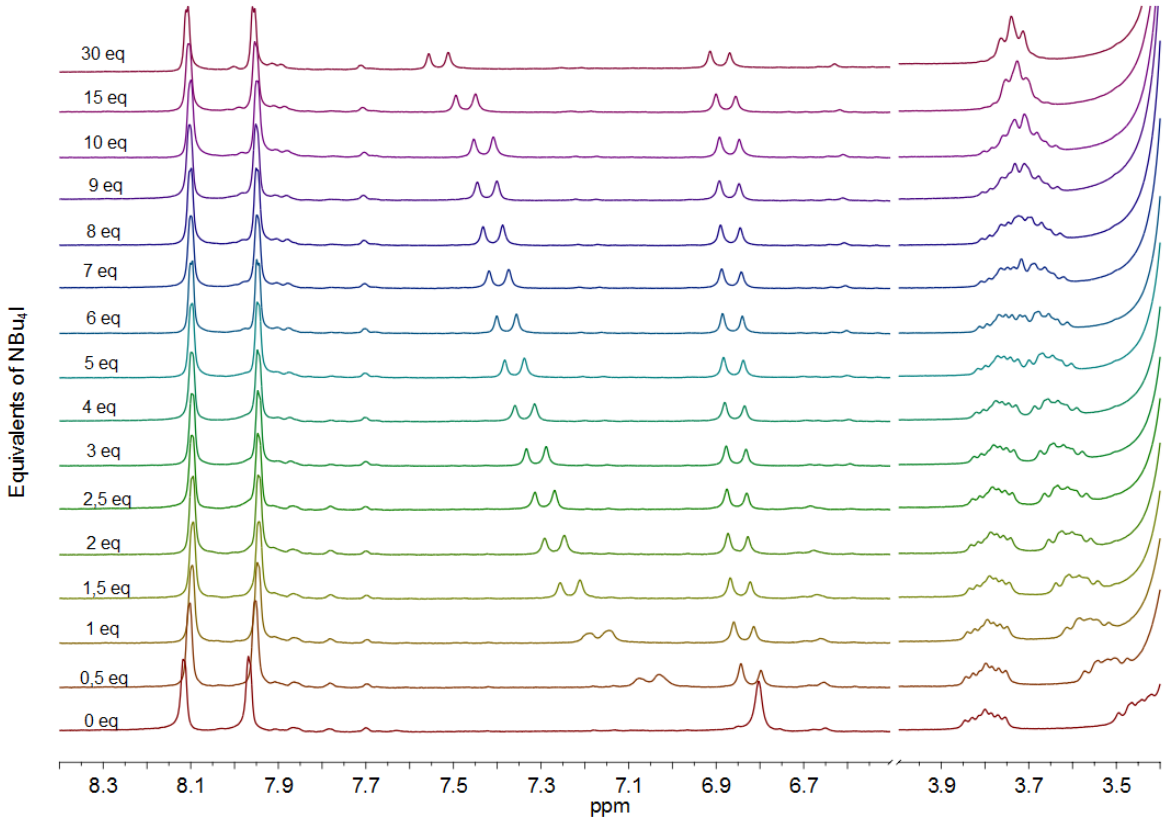

Figure S14: ^{1}H NMR titration (300 MHz, 298 K) of Bu_4NI in DMSO-d_6 into a $3.90 \cdot 10^{-3}$ M solution of **$[AuL^3_2](PF_6)_3$** in DMSO-d_6.

Table S3: ^{1}H NMR titration (300 MHz, 298 K) data of Bu_4NI in DMSO-d_6 into a $3.90 \cdot 10^{-3}$ M solution of **$[AuL^3_2](PF_6)_3$** in DMSO-d_6.

$[Au]_0$ (mM)	$[I^-]_0$ (mM)	$[I^-]_0/[Au]_0$	δ HA (ppm)	Δδ HA (ppm)	δ CH_2 X A (ppm)	δ CH_2 X B (ppm)
3.900	0.000	0.0	6.803	0	nd	nd
3.881	1.943	0.5	7.053	0.232	3.4351	3.7998
3.861	3.867	1.0	7.164	0.327	3.5122	3.7988
3.842	5.772	1.5	7.234	0.39	3.5555	3.7944
3.824	7.659	2.0	7.269	0.437	3.5914	3.7897
3.805	9.527	2.5	7.29	0.438	3.6026	3.7876
3.786	11.38	3.0	7.31	0.456	3.622	3.7844
3.750	15.02	4.0	7.336	0.478	3.6314	3.7801
3.714	18.60	5.0	7.36	0.5	3.6426	3.7754
3.679	22.11	6.0	7.378	0.516	3.6586	3.7567
3.645	25.55	7.0	7.396	0.532	3.6838	3.7383
3.611	28.93	8.0	7.409	0.543	3.6923	3.739
3.578	32.25	9.0	7.424	0.553	3.6941	3.7406
3.545	35.51	10.0	7.431	0.561	3.6952	3.7395
3.391	50.95	15.0	7.474	0.593	3.696	3.7387
3.000	90.14	30.0	7.534	0.642	3.7272	3.7272

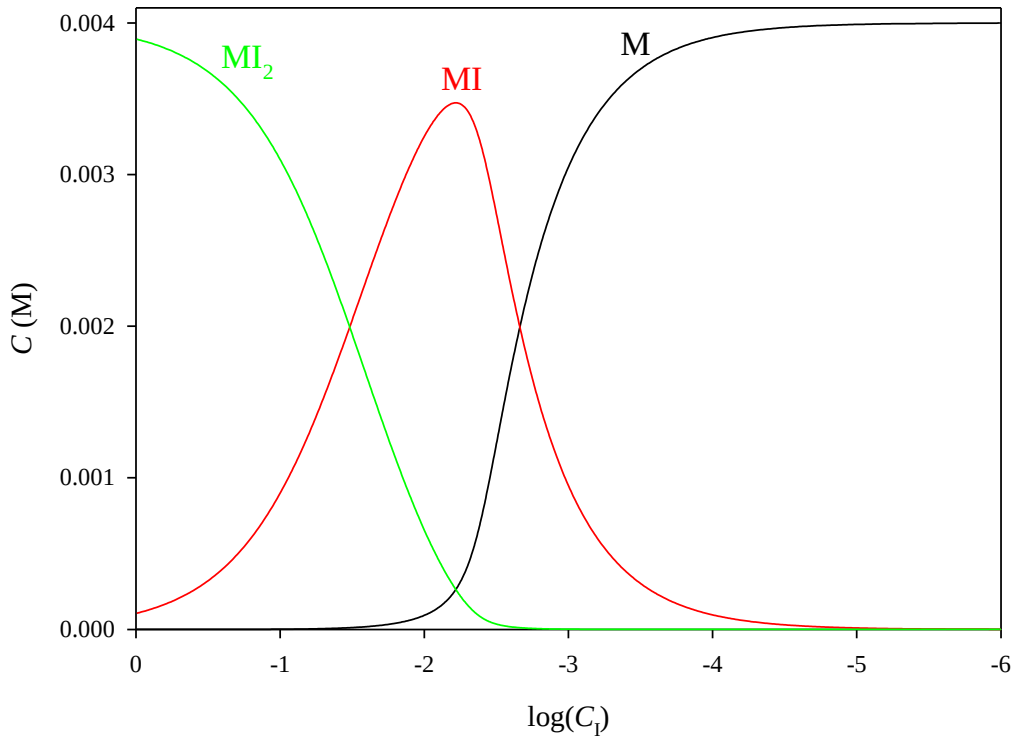

Figure S15: Species distribution diagram versus the total concentration of iodide for 0.0004 M host solution (M = $\mathbf{[AuL^3{}_2]^{3+}}$, MI = $\mathbf{[AuIL^3{}_2]^{2+}}$, MI_2 = $\mathbf{[AuI_2L^3{}_2]^{+}}$).

7. NMR titration of $Et_4NCl{\cdot}H_2O$ to $[AuL^4{}_2](PF_6)_3$ in DMSO-d_6 (*Method B*)

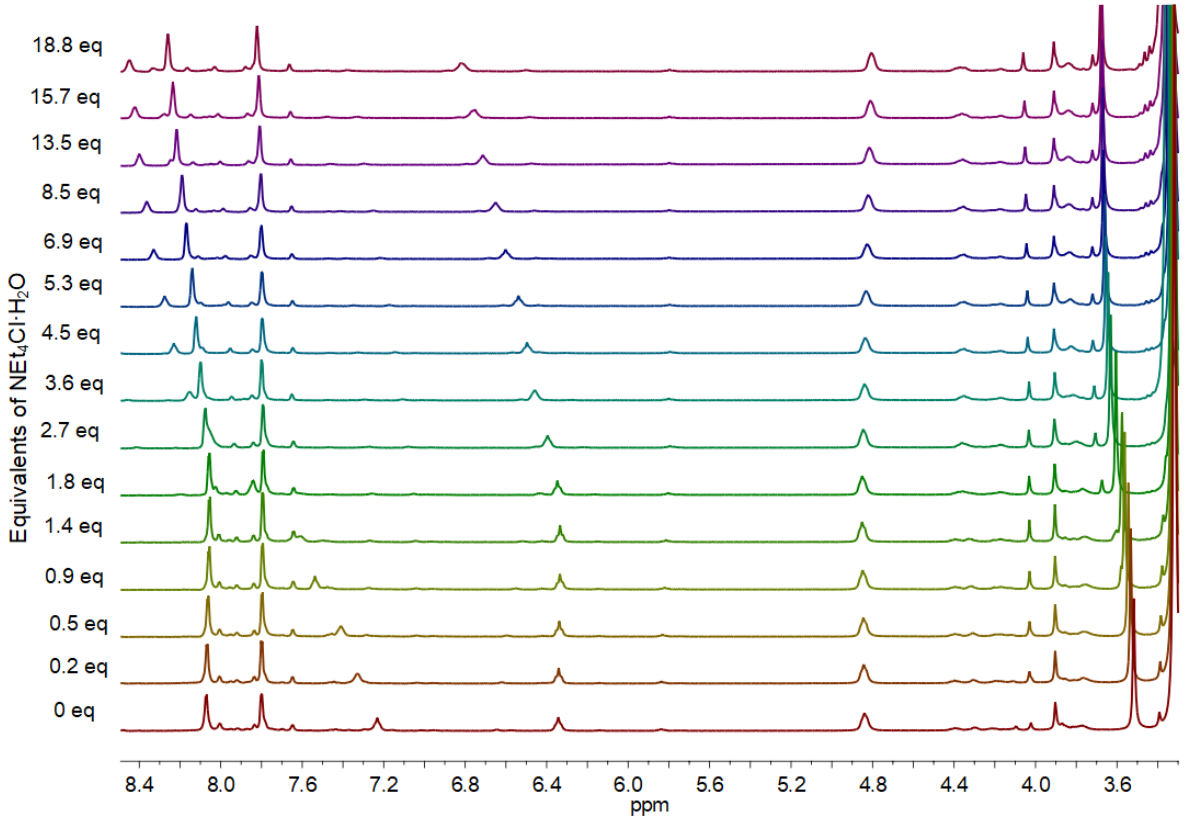

Figure S16: ^{1}H NMR titration (300 MHz, 298 K) of $Et_4NCl{\cdot}H_2O$ in DMSO-d_6 into a $7.28{\cdot}10^{-3}$ M solution of **$[AuL^4{}_2](PF_6)_3$** in DMSO-d_6.

Table S4: ^{1}H NMR titration (300 MHz, 298 K) data of $Et_4NCl{\cdot}H_2O$ in DMSO-d_6 into a $7.28{\cdot}10^{-3}$ M solution of **$[AuL^4{}_2](PF_6)_3$** in DMSO-d_6.

$[Au]_0$ (mM)	$[Cl^-]_0$ (mM)	$[Cl^-]_0/[Au]_0$	δ *CH* [ppm]	δ *OH* [ppm]	δ CH_3[ppm]
7.28	0	0.0	7.231	6.343	3.518
7.28	1.69	0.2	7.329	6.341	3.532
7.28	3.38	0.5	7.410	6.338	3.544
7.28	6.72	0.9	7.538	6.336	3.562
7.28	10.0	1.4	7.606	6.334	3.575
7.28	13.3	1.8	7.843	6.347	3.606
7.28	19.8	2.7	8.055	6.396	3.631
7.28	26.2	3.6	8.150	6.458	3.643
7.28	32.4	4.5	8.230	6.496	3.665
7.28	38.5	5.3	8.276	6.538	3.660
7.28	50.5	6.9	8.330	6.602	3.666
7.28	62.0	8.5	8.363	6.660	3.669
7.28	89.2	13.5	8.400	6.713	3.673
7.28	114.0	15.7	8.419	6.752	3.675
7.28	137.0	18.8	8.447	6.823	3.678

8. NMR titration of Et_4NBr to $[AuL^4_2](PF_6)_3$ in DMSO-d_6 (*Method B*)

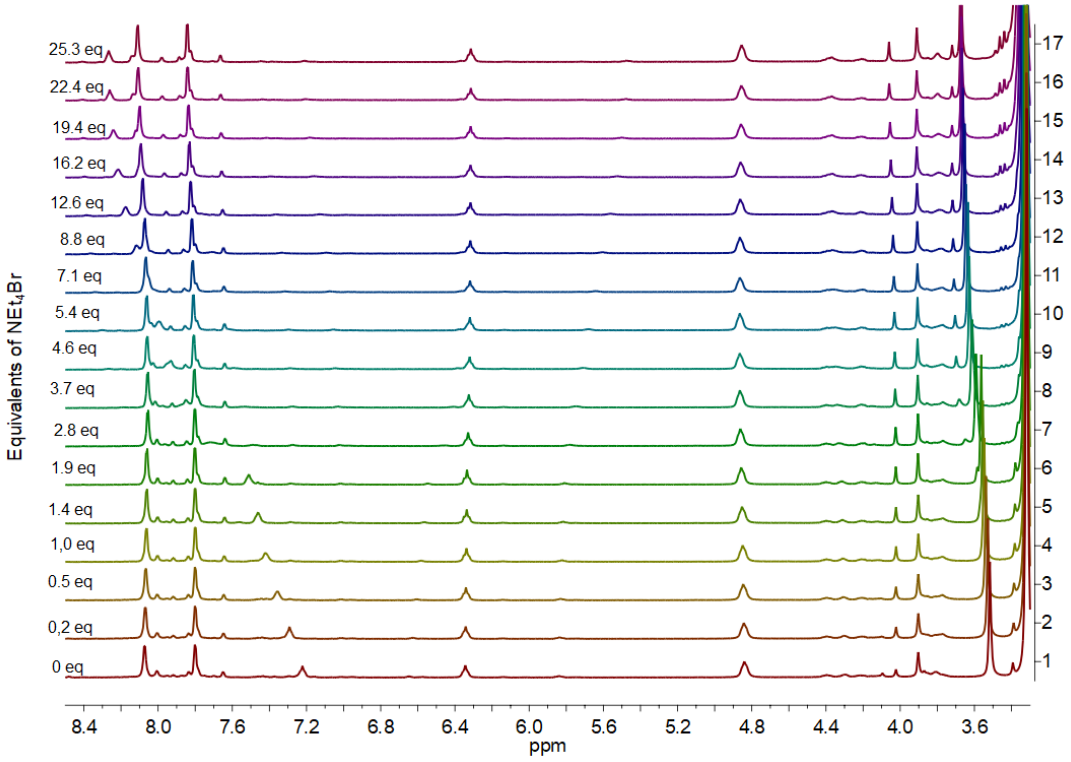

Figure S17: ^{1}H NMR titration (300 MHz, 298 K) of Et_4NBr in DMSO-d_6 into a $7.05 \cdot 10^{-3}$ M solution of **$[AuL^4_2](PF_6)_3$** in DMSO-d_6.

Table S5: ^{1}H NMR titration (300 MHz, 298 K) data of Et_4NBr in DMSO-d_6 into a $7.05 \cdot 10^{-3}$ M solution of **$[AuL^4_2](PF_6)_3$** in DMSO-d_6.

$[Au]_0$ (mM)	$[Br^-]_0$ (mM)	$[Br^-]_0/[Au]_0$	δ C*H* [ppm]	δ O*H* [ppm]	δ CH_3 [ppm]
7.05	0	0.0	7.222	6.344	3.517
7.05	1.69E-03	0.2	7.291	6.342	3.527
7.05	3.37E-03	0.5	7.355	6.340	3.538
7.05	6.70E-03	1.0	7.423	6.338	3.547
7.05	1.00E-02	1.4	7.461	6.337	3.555
7.05	1.33E-02	1.9	7.510	6.336	3.563
7.05	1.97E-02	2.8	7.718	6.329	3.592
7.05	2.61E-02	3.7	7.848	6.325	3.612
7.05	3.23E-02	4.6	7.933	6.321	3.627
7.05	3.84E-02	5.4	7.991	6.319	3.634
7.05	5.03E-02	7.1	8.050	6.318	3.645
7.05	6.18E-02	8.8	8.119	6.317	3.653
7.05	8.89E-02	12.6	8.173	6.316	3.661
7.05	1.14E-01	16.2	8.214	6.316	3.667
7.05	1.37E-01	19.4	8.241	6.315	3.670
7.05	1.58E-01	22.4	8.261	6.314	3.672
7.05	1.78E-01	25.3	8.266	6.315	3.672

9. NMR titration of Bu_4NI to $[AuL^4_2](PF_6)_3$ in DMSO-d_6 (*Method B*)

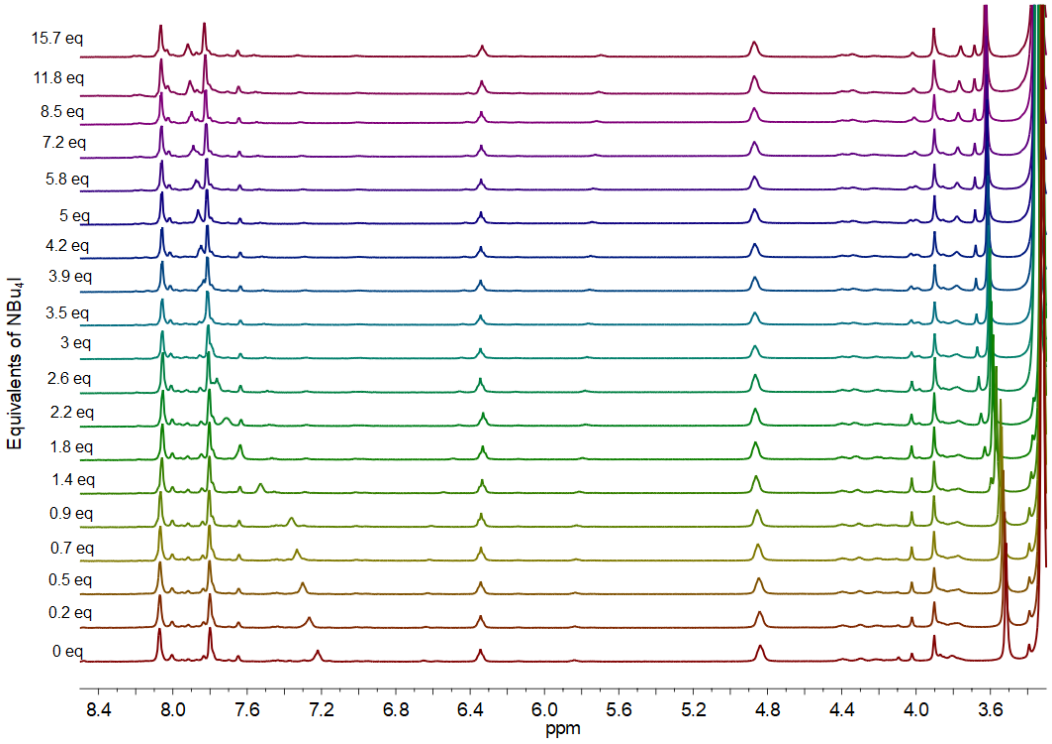

Figure S18: ^{1}H NMR titration (300 MHz, 298 K) of Bu_4NI in DMSO-d_6 into a $7.05 \cdot 10^{-3}$ M solution of **$[AuL^3_2](PF_6)_3$** in DMSO-d_6.

Table S6: ^{1}H NMR titration (300 MHz, 298 K) data of Bu_4NI in DMSO-d_6 into a $7.05 \cdot 10^{-3}$ M solution of **$[AuL^4_2](PF_6)_3$** in DMSO-d_6.

$[Au]_0$ (mM)	$[I^-]_0$ (mM)	$[I^-]_0/[Au]_0$	δ *CH* [ppm]	δ O*H* [ppm]	δ CH_3 [ppm]
7.05	0	0.0	7.220	6.344	3.516
7.05	1.63E-03	0.2	7.266	6.344	3.523
7.05	3.25E-03	0.5	7.301	6.343	3.531
7.05	4.85E-03	0.7	7.333	6.342	3.539
7.05	6.44E-03	0.9	7.360	6.341	3.545
7.05	9.57E-03	1.4	7.528	6.335	3.569
7.05	1.27E-02	1.8	7.637	6.332	3.585
7.05	1.57E-02	2.2	7.713	6.330	3.596
7.05	1.86E-02	2.6	7.763	6.345	3.602
7.05	2.15E-02	3.0	7.797	6.344	3.607
7.05	2.44E-02	3.5	7.815	6.344	3.610
7.05	2.72E-02	3.9	7.834	6.344	3.612
7.05	2.99E-02	4.2	7.847	6.343	3.614
7.05	3.54E-02	5.0	7.865	6.342	3.617
7.05	4.06E-02	5.8	7.876	6.341	3.619
7.05	5.05E-02	7.2	7.889	6.340	3.621
7.05	5.98E-02	8.5	7.899	6.340	3.623
7.05	8.33E-02	11.8	7.908	6.338	3.625
7.05	1.11E-01	15.7	7.919	6.336	3.627

10. Titration curves for $[AuL^4_2](PF_6)_3$ in DMSO-d_6

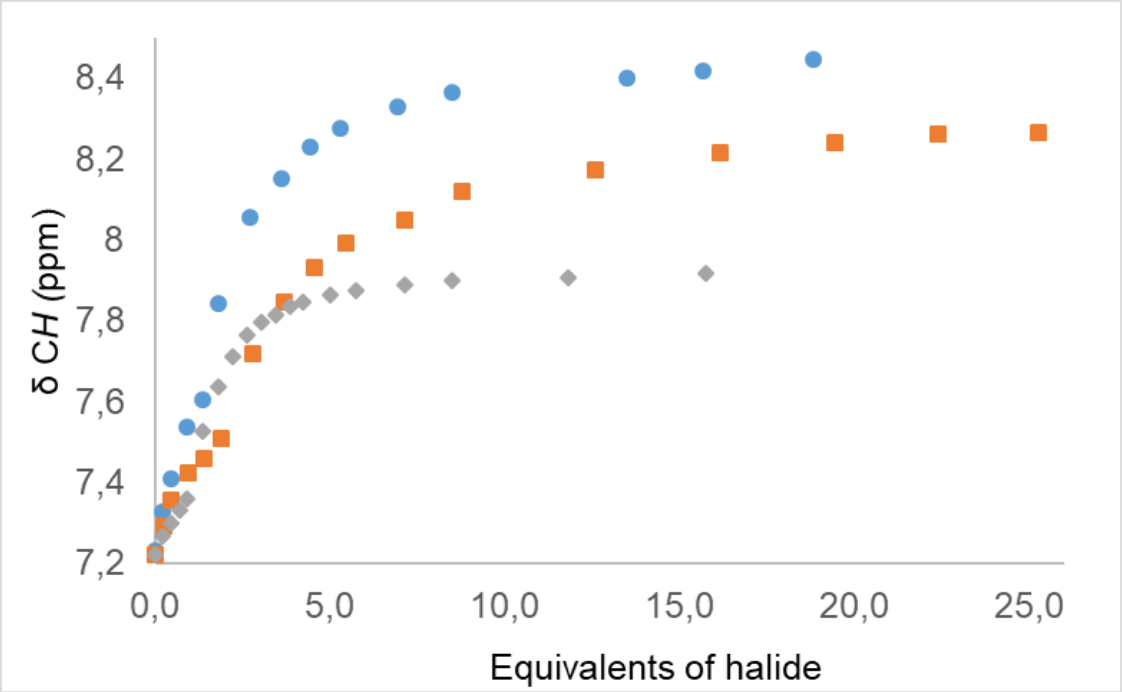

Figure S19: Titration curves for **$[AuL^4_2](PF_6)_3$** in dmso-d_6 with chloride (blue), bromide (orange) and iodide (grey).

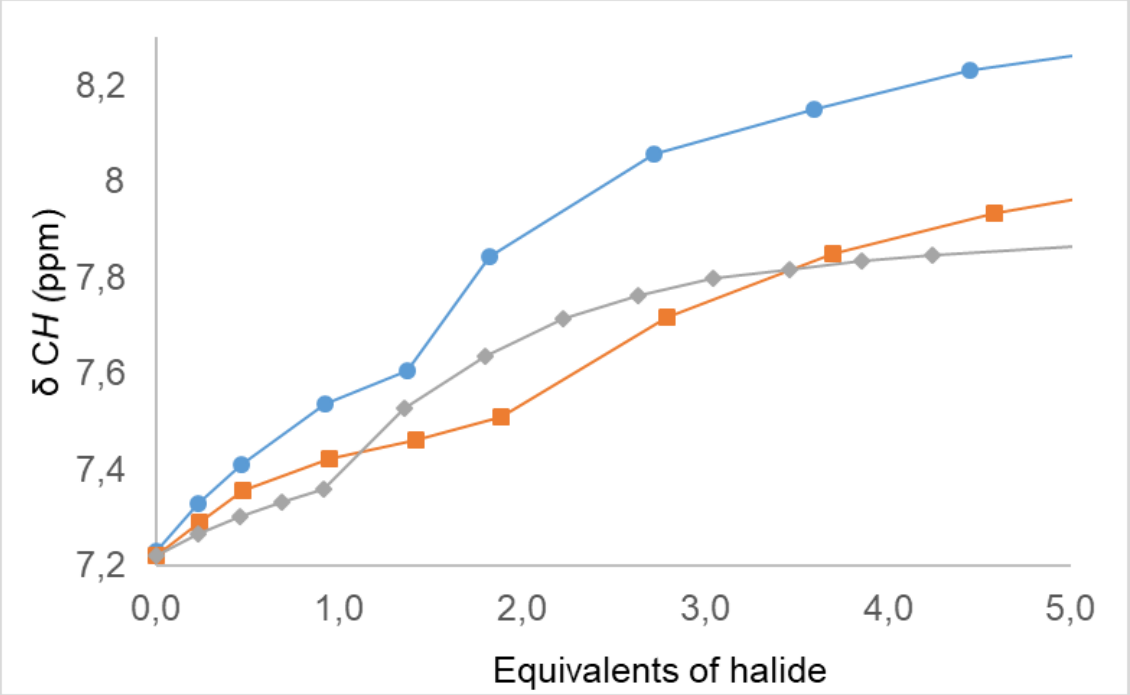

Figure S20: Titration curves for **$[AuL^4_2](PF_6)_3$** in DMSO-d_6 with chloride (blue), bromide (orange) and iodide (grey), magnification of the part of the curves between 0 and 5 equivalents of halide. Lines are only guide for the eyes.

11. NMR titration of $NEt_4Cl \cdot H_2O$ to $[AuL^4_2](PF_6)_3$ in D_2O (*Method B*)

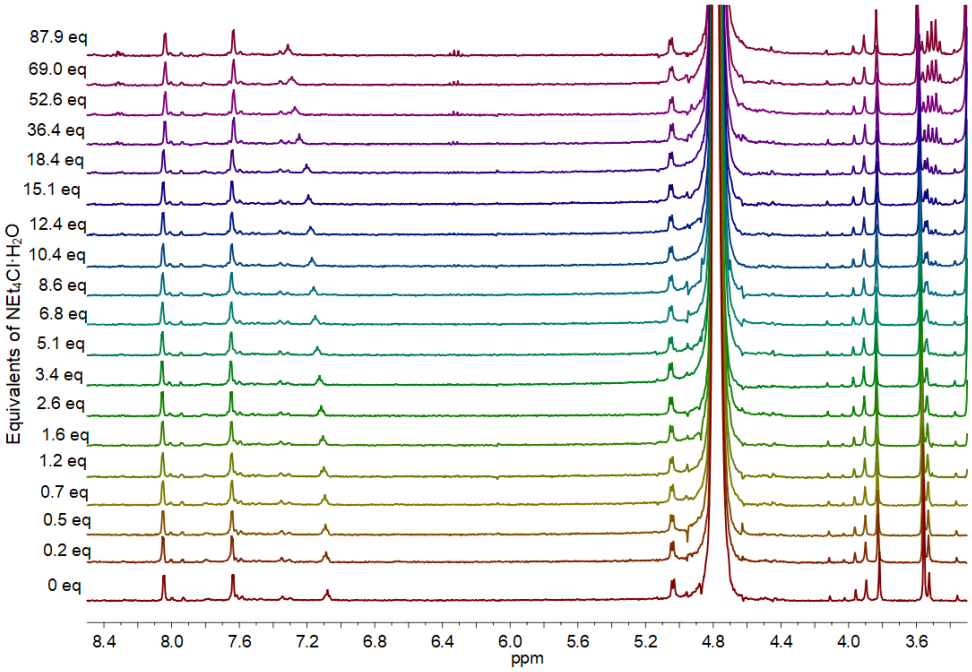

Figure S21: ^{1}H NMR titration (300 MHz, 298 K) of $Et_4NCl \cdot H_2O$ in D_2O into a $0.61 \cdot 10^{-3}$ M solution of **$[AuL^4_2](PF_6)_3$** in D_2O.

Table S7: ^{1}H NMR titration (300 MHz, 298 K) data of $Et_4NCl \cdot H_2O$ in D_2O into a $0.61 \cdot 10^{-3}$ M solution of **$[AuL^4_2](PF_6)_3$** in D_2O.

$[Au]_0$ (mM)	$[Cl^-]_0$ (mM)	$[Cl^-]_0/[Au]_0$	δ *CH* [ppm]
0.61	0.00	0,0	7.079
0.61	0.144	0,2	7.087
0.61	0.287	0,5	7.091
0.61	0.429	0,7	7.096
0.61	0.712	1,2	7.101
0.61	0.992	1,6	7.106
0.61	1.58	2,6	7.117
0.61	2.09	3,4	7.126
0.61	3.14	5,1	7.139
0.61	4.16	6,8	7.151
0.61	5.27	8,6	7.162
0.61	6.33	10,4	7.171
0.61	7.58	12,4	7.181
0.61	9.19	15,1	7.192
0.61	11.2	18,4	7.204
0.61	22.2	36,4	7.246
0.61	32.1	52,6	7.272
0.61	42.1	69,0	7.289
0.61	53.6	87,9	7.313

12. NMR titration of Bu_4NI to $[AuL^4_2](PF_6)_3$ in D_2O (*Method B*)

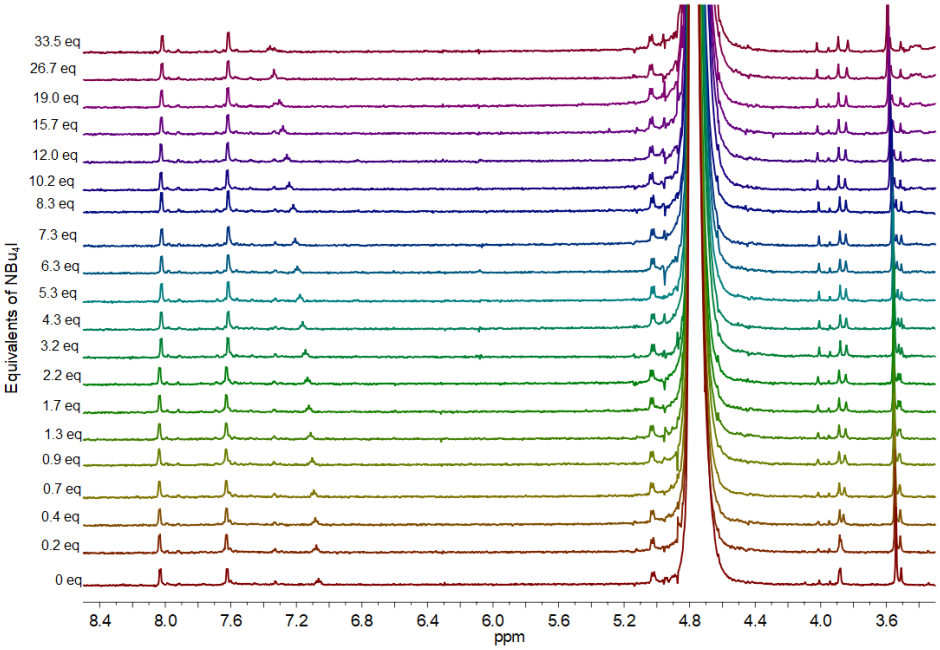

Figure S22: ^{1}H NMR titration (300 MHz, 298 K) of Bu_4NI in D_2O into a $0.69 \cdot 10^{-3}$ M solution of **$[AuL^4_2](PF_6)_3$** in D_2O.

Table S8: ^{1}H NMR titration (300 MHz, 298 K) data of Bu_4NI in D_2O into a $7.05 \cdot 10^{-3}$ M solution of **$[AuL^4_2](PF_6)_3$** in D_2O.

$[Au]_0$ (mM)	$[I^-]_0$ (mM)	$[I^-]_0/[Au]_0$	δ *CH* [ppm]
0.69	0.00	0.0	7.066
0.69	0.151	0.2	7.079
0.69	0.302	0.4	7.085
0.69	0.452	0.7	7.094
0.69	0.602	0.9	7.103
0.69	0.899	1.3	7.113
0.69	1.20	1.7	7.124
0.69	1.49	2.2	7.132
0.69	2.22	3.2	7.145
0.69	2.94	4.3	7.161
0.69	3.64	5.3	7.178
0.69	4.34	6.3	7.196
0.69	5.03	7.3	7.207
0.69	5.70	8.3	7.219
0.69	7.03	10.2	7.243
0.69	8.31	12.0	7.258
0.69	10.8	15.7	7.282
0.69	13.1	19.0	7.305
0.69	18.4	26.7	7.337
0.69	23.1	33.5	7.360

13. Titration curves for $[AuL^4_2](PF_6)_3$ in D_2O

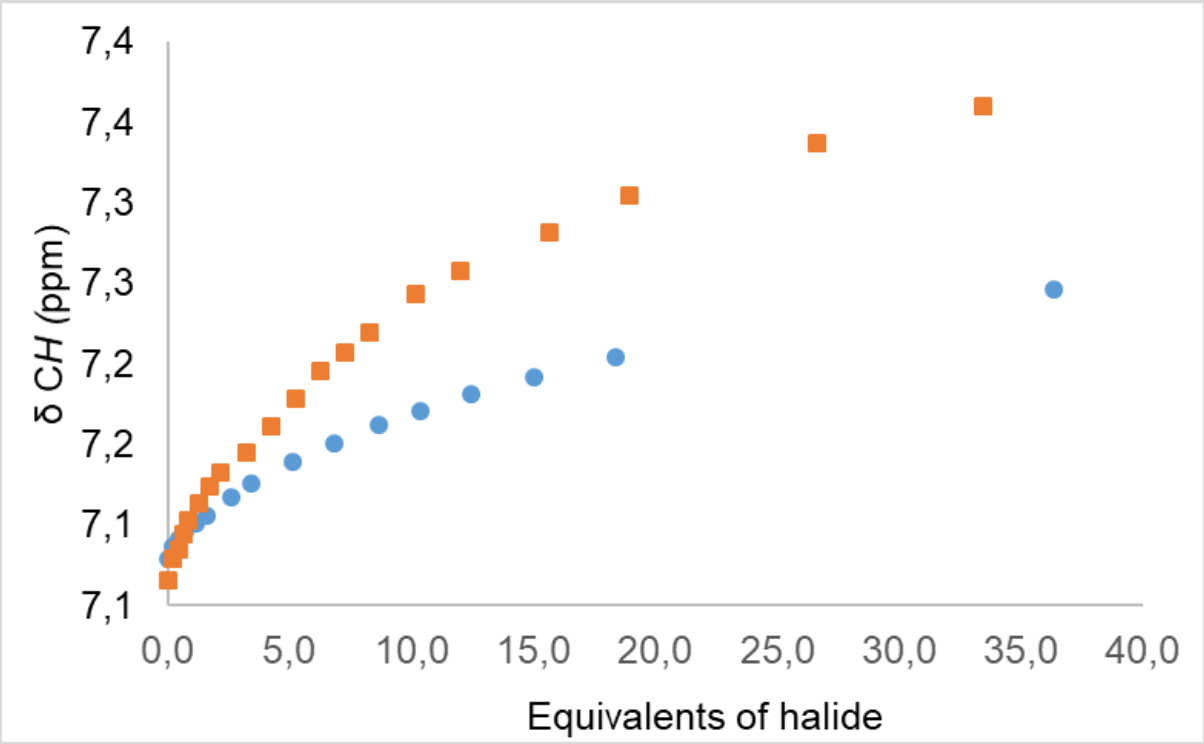

Figure S23: Titration curves for **$[AuL^4_2](PF_6)_3$** in D_2O with chloride (blue) and iodide (orange).

Table S9. Formation constants for the species $[AuXL_2]^{2+}$, $[AuX_2L_2]^{+}$, $[AuL_2X_3]$ and $[AuL_2X_4]^{-}$

Solvent	Complex	Anion	Log β $[AuL_2X]^{2+}$	Log β $[AuL_2X_2]^{+}$	Log β $[AuL_2X_3]$	Log β $[AuL_2X_4]^{-}$
DMSO-d_6	**$[AuL^4_2]^{3+}$**	Cl^-	1.5 ± 0.01	5.66 ± 0.01	7.83 ± 0.01	8.78 ± 0.01
DMSO-d_6	**$[AuL^4_2]^{3+}$**	Br^-	3.77 ± 0.01	9.27 ± 0.01	11.33 ± 0.01	11.19 ± 0.01
DMSO-d_6	**$[AuL^4_2]^{3+}$**	I^-	5.54 ± 0.01	7.59 ± 0.01	8.95 ± 0.01	11.84 ± 0.01
D_2O	**$[AuL^4_2]^{3+}$**	Cl^-	3.74 ± 0.01	5.71± 0.01	7.64± 0.01	8.07± 0.01
D_2O	**$[AuL^4_2]^{3+}$**	I^-	3.57± 0.01	4.70± 0.01	8.55± 0.01	9.92± 0.01
DMSO-d_6	**$[AuL^1_2]^{3+}$**	Cl^-	4.062 ± 0.093	6.390 ± 0.097		
DMSO-d_6	**$[AuL^1_2]^{3+}$**	Br^-	3.685 ± 0.074	5.775 ± 0.075		
DMSO-d_6	**$[AuL^1_2]^{3+}$**	I^-	2.552 ± 0.045	3.876 ± 0.075		
D_2O	**$[AuL^1_2]^{3+}$**	Cl^-	1.67 ± 0.02	-	-	-
D_2O	**$[AuL^1_2]^{3+}$**	I^-	2.16 ± 0.02	-	-	-

Data for compound **$[AuL^1_2]^{3+}$** reported in [1]

14. UV-vis titration of $Et_4NCl \cdot H_2O$ to $[AuL^3_2](PF_6)_3$ in DMSO

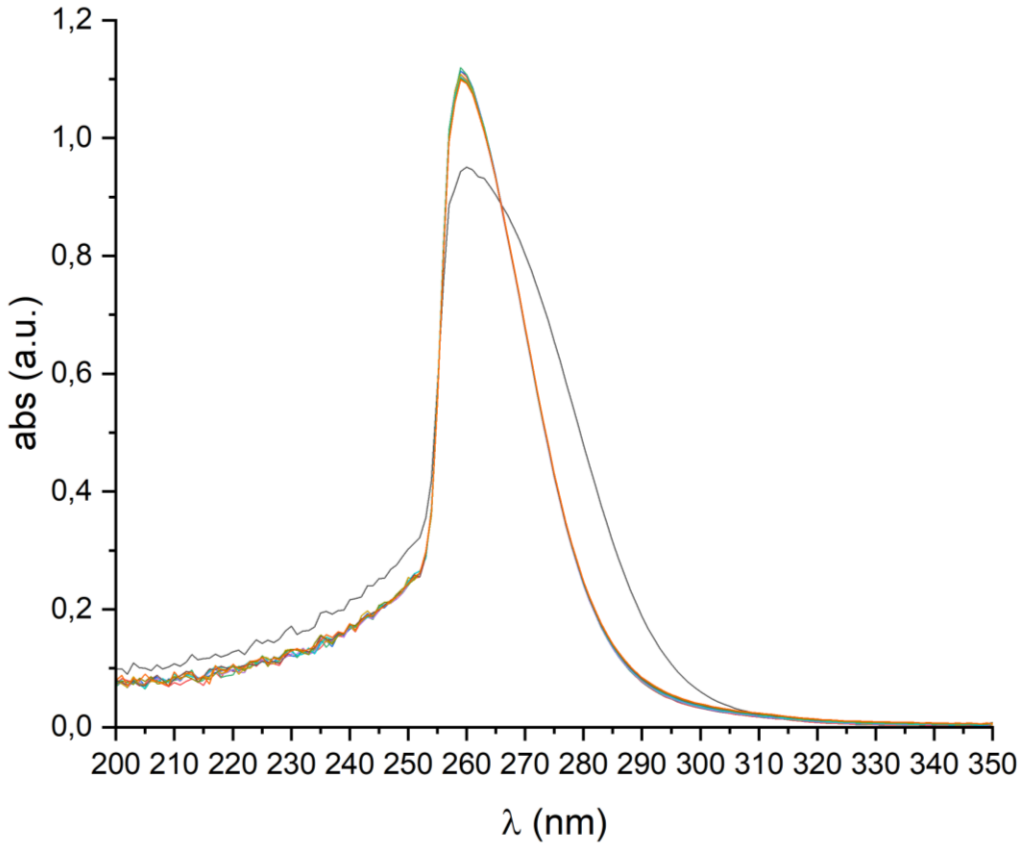

Figure S24: UV-vis titration (298 K) of $Et_4NCl \cdot H_2O$ in DMSO into a $5.00 \cdot 10^{-5}$ M solution of **$[AuL^3_2](PF_6)_3$** in DMSO.

Table S10: UV-vis titration (298 K) of Et_4NCl in DMSO into a $5.00 \cdot 10^{-5}$ M solution of **$[AuL^3_2](PF_6)_3$** in DMSO.

$[Au]_0$ ($\cdot 10^{-5}$ M)	$[Cl^-]_0$ ($\cdot 10^{-5}$ M)	Abs 320 nm (a.u.)
5.00	0.00	0.0125
5.00	9.54	0.0153
5.00	19.00	0.0157
5.00	28.40	0.0163
5.00	37.70	0.0176
5.00	47.00	0.0163
5.00	56.10	0.0167
5.00	65.20	0.0168
5.00	74.30	0.0172
5.00	83.20	0.0167
5.00	92.10	0.0193
5.00	114.00	0.0193
5.00	136.00	0.0184
5.00	157.00	0.0207
5.00	177.00	0.0187
5.00	365.00	0.0198

15. UV-vis titration of Et_4NBr to $[AuL^3_2](PF_6)_3$ in DMSO

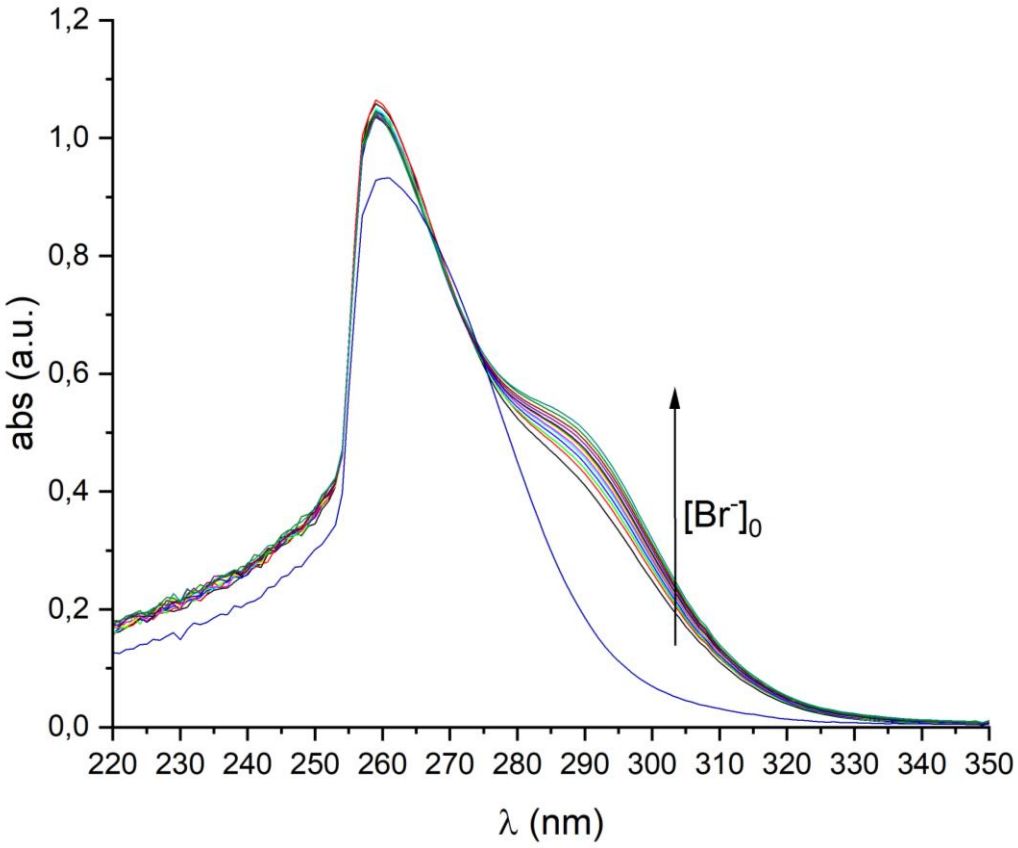

Figure S25: UV-vis titration (298 K) of Et_4NBr in DMSO into a $5.00 \cdot 10^{-5}$ M solution of $\mathbf{[AuL^3_2](PF_6)_3}$ in DMSO.

Table S11: UV-vis titration (298 K) of Et_4NBr in DMSO into a $5.00 \cdot 10^{-5}$ M solution of $\mathbf{[AuL^3_2](PF_6)_3}$ in DMSO.

$[Au]_0$ ($\cdot 10^{-5}$ M)	$[Br^-]_0$ ($\cdot 10^{-5}$ M)	Abs 292 nm (a.u.)
5.00	0.0	0,152
5.00	73.5	0.382
5.00	146.0	0.402
5.00	216.0	0.411
5.00	285.0	0.420
5.00	353.0	0.429
5.00	420.0	0.433
5.00	550.0	0.440
5.00	613.0	0.442
5.00	675.0	0.445
5.00	795.0	0.454
5.00	912.0	0.461
5.00	1020.0	0.468
5.00	1240.0	0.477

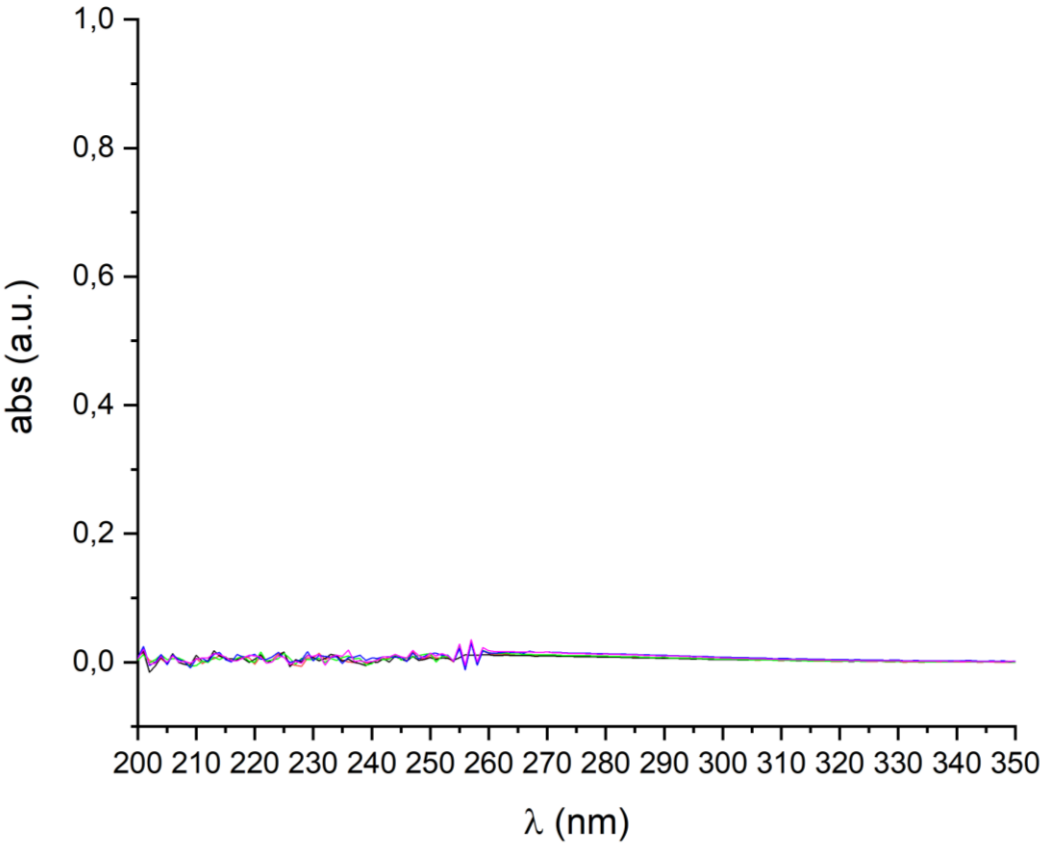

Figure S26: UV-vis spectra (298 K) of Et_4NBr in DMSO at increasing concentrations.

Table S12: UV-vis spectra (298 K) of Bu_4NBr in DMSO at increasing concentrations.

$[Br^-]_0$ ($\cdot 10^{-5}$ M)	Abs 292 nm (a.u.)
0.0	0.0
256	0.00643
493	0.00601
714.0	0.00673
919.0	0.00101
1110.0	0.00949

16. UV-vis titration of Bu_4NI to $[AuL^3_2](PF_6)_3$ in DMSO

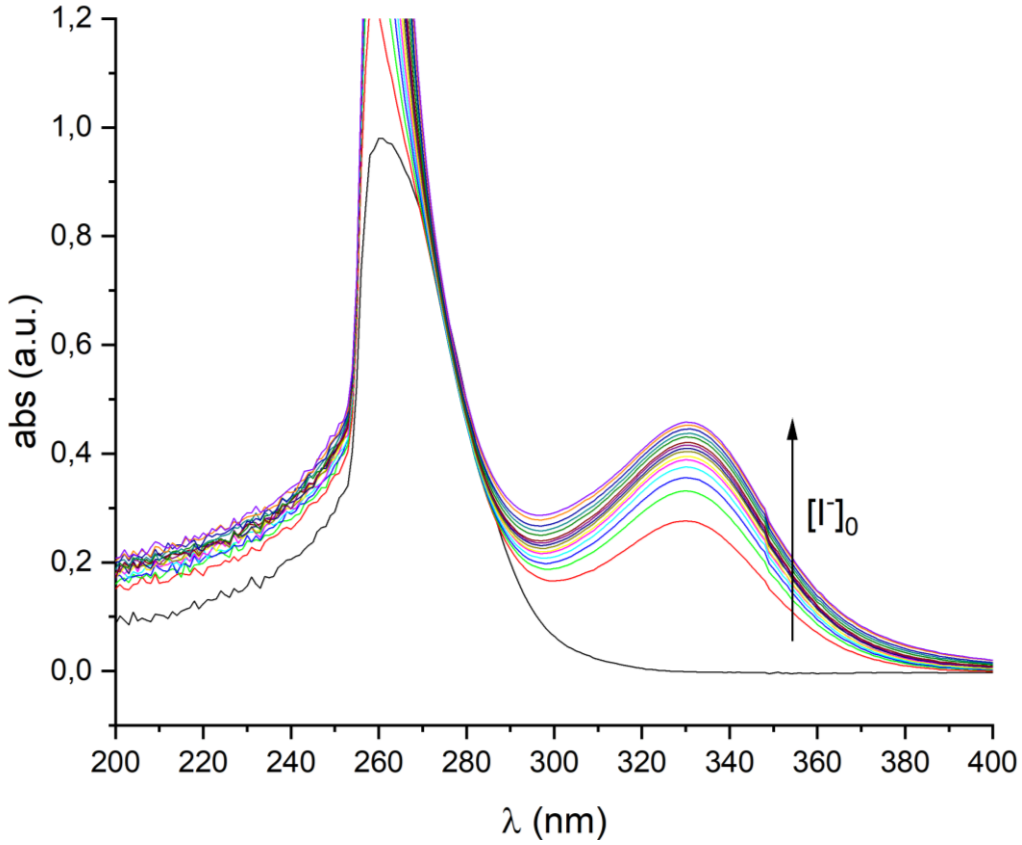

Figure S27: UV-vis titration (298 K) of Bu_4NI in DMSO into a $5.00 \cdot 10^{-5}$ M solution of **$[AuL^3_2](PF_6)_3$** in DMSO.

Table S13: UV-vis titration (298 K) of Bu_4NI in DMSO into a $5.00 \cdot 10^{-5}$ M solution of **$[AuL^3_2](PF_6)_3$** in DMSO.

$[Au]_0$ ($\cdot 10^{-5}$ M)	$[I^-]_0$ ($\cdot 10^{-5}$ M)	Abs 330 nm (a.u.)
5.00	0.0	0.0
5.00	59.0	0.277
5.00	117.0	0.331
5.00	173.0	0.356
5.00	229.0	0.375
5.00	284.0	0.389
5.00	337.0	0.395
5.00	390.0	0.403
5.00	441.0	0.409
5.00	492.0	0.416
5.00	541.0	0.421
5.00	638.0	0.430
5.00	731.0	0.437
5.00	822.0	0.445
5.00	909.0	0.452
5.00	993.0	0.458

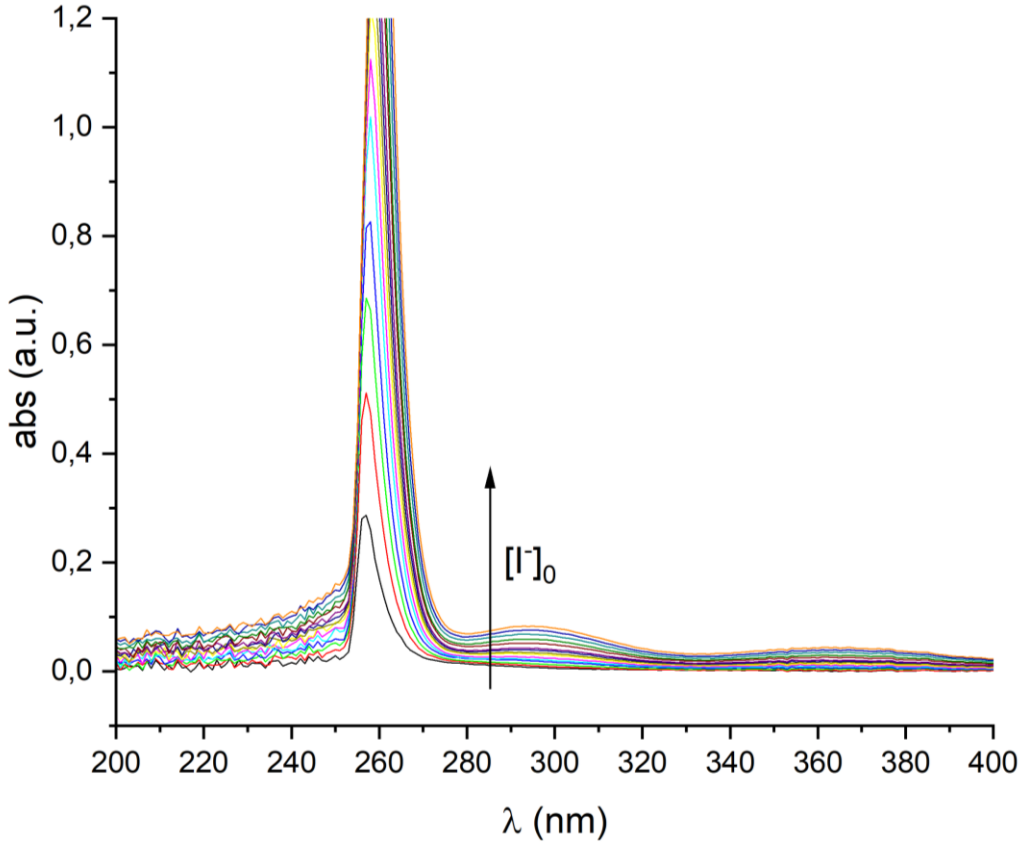

Figure S28: UV-vis spectra (298 K) of Bu_4NI in DMSO at increasing concentrations.

Table S14: UV-vis spectra (298 K) of Bu_4NI in DMSO at increasing concentrations.

$[I^-]_0$ ($\cdot 10^{-5}$ M)	Abs 330 nm (a.u.)
0.0	0.0
59.0	0.00156
117.0	0.00244
173.0	0.00376
229.0	0.0059
284.0	0.00717
337.0	0.00889
390.0	0.0106
441.0	0.01227
492.0	0.01359
541.0	0.0154
638.0	0.01904
731.0	0.02092
822.0	0.02495
909.0	0.02812
993.0	0.03213

17. Crystallographic data

Table S15. Crystal data for compounds.

Compound	**[AuL$^3_2$](PF$_6$)$_3$**	**[AuL$^4_2$](PF$_6$)$_3$**	**[Au$_2$L$^5_2$](PF$_6$)$_2$**	**[AuBr(L^7)(L^{7}O)](BF$_4$)$_2$**
Formula	$C_{32}H_{51}AuF_{18}N_9P_3$	$C_{22}H_{31}AuF_{18}N_9O_2P_3$	$C_{65}H_{106}Au_4Cl_{10}F_{24}N_{16}P_4$	$C_{42}H_{44}AuB_2BrF_8N_{12}O$
Molecular Weight	1193.69	1085.43	2833.90	1183.38
Crystal system	Triclinic	Monoclinic	Monoclinic	Triclinic
Space group	*P* -1	*C* 2/c	*P* 2$_1$/c	*P* -1
a[Å]	11.0145(2)	22.016(3)	14.2720(13)	12.4565(5)
b[Å]	11.6955(2)	17.330(3)	18.403(2)	12.7075(7)
c[Å]	19.4594(4)	10.6014(17)	20.5222(19)	15.2901(9)
α[°]	91.277(2)	90	90	95.188(5)
β[°]	91.719(2)	116.972(2)	108.341(4)	100.081(4)
γ[°]	117.298(3)	90	90	2.521(4)
V[Å^3]	2224.75(9)	3604.8(10)	5116.4(9)	2368.7(2)
Temperature (K)	293	273	299	173
Z	2	4	2	2
D_{calc}[g·cm^{-3}]	1.782	2.000	1.839	1.659
μ[cm^{-1}]	3.527	4.346	6.129	4.028
F(000)	1184.0	2112.0	2740.0	1168.0
Reflections collected	32907	19472	126439	27486
Independent reflections	11789	3968	10515	9313
Reflections in refinement	8824	3262	7043	7766
R(int)	0.0453	0.0523	0.0896	0.0511
Refined parameters	576	256	535	558
R_1 [$I > 2\sigma(I)$]	R_1 = 0.0303 wR_2 = 0.0713	R_1 = 0.0354 wR_2 = 0.0934	R_1 = 0.0966 wR_2 = 0.2250	R_1 = 0.0488 wR_2 =0.1389
wR_2 [all data]	R_1 = 0.0461 wR_2 = 0.0813	R_1 = 0.0440 wR_2 = 0.0979	R_1 = 0.1408 wR_2 = 0.2553	R_1 = 0.0626 wR_2 =0.1487
GOF	0.866	1.046	1.059	1.050
CCDC	1964958	1964960	1964955	1964956

$R_1 = \Sigma|Fo-Fc|/\Sigma(Fo)$; $wR_2 = [\Sigma[w(Fo^2-Fc^2)^2]/\Sigma[w(Fo^2)^2]]^{1/2}$.

Table S16: Crystal data for compounds.

Compound	$[AuL^3_2](Br)_2(Br_3)$	$[AuL^3_2](I_3)_3$	$[AuL^4_2]Cl_3$
Formula	$C_{32}H_{51}AuBr_5N_9$	$C_{64}H_{106}Au_2I_{18}N_{16}O$	$C_{24}H_{40}AuCl_3N_8O_4S_2$
Molecular Weight	1158.33	3793.79	872.07
Crystal system	Monoclinic	Monoclinic	triclinic
Space group	*C* 2/c	*P* 2_1/n	*P-1*
a[Å]	25.004(2)	9.281(3)	10.2116(7)
b[Å]	10.2313(8)	14.603(4)	11.6009(8)
c[Å]	15.9405(15)	20.213(6)	14.6925(10)
α[°]	90	90	82.052(2)
β[°]	92.050(2)	90.385(5)	81.090(2)
γ[°]	90	90	72.743(2)
V[Å^3]	4075.3(6)	2739.4(14)	1634.2(2)
Temperature (K)	173	296	100.91
Z	4	1	2
D_{calc}[g·cm^{-3}]	1.888	2.300	1.772
μ[cm^{-1}]	8.547	7.786	4.918
F(000)	2240.0	1722.0	868.0
Reflections collected	32734	31556	124019
Independent reflections	6334	5495	8155
Reflections in refinement	5158	4043	8155
R(int)	0.0434	0.0856	0.0282
Refined parameters	253	237	393
R_1 [$I > 2\sigma(I)$]	R_1 = 0.0260 wR_2 = 0.0610	R_1 = 0.0536 wR_2 =0.1493	0.0179 0.0386
wR_2 [all data]	R_1 = 0.0368 wR_2 = 0.0653	R_1 = 0.0708 wR_2 =0.1562	0.0213 0.0398
GOF	0.923	1.006	1.080
CCDC	1964957	1964959	1964961

$R_1 = \Sigma||Fo-Fc|/\Sigma(Fo)$; $wR_2 = [\Sigma[w(Fo^2-Fc^2)^2]/\Sigma[w(Fo^2)^2]]^{1/2}$.

18. References

1 M. Baron, A. Dall'Anese, C. Tubaro, L. Orian, V. D. Marco, S. Bogialli, C. Graiff and M. Basato, *Dalton Trans.*, 2018, **47**, 935–945.